The Structure of the Carboxyl Terminus of Striated α-Tropomyosin in Solution Reveals an Unusual Parallel Arrangement of Interacting α-Helices[†,‡]

Norma J. Greenfield,[*,§] G. V. T. Swapna,[||] Yuanpeng Huang,[||] Thomas Palm,[§] Sarah Graboski,[§] Gaetano T. Montelione,[||] and Sarah E. Hitchcock-DeGregori[§]

Department of Neuroscience and Cell Biology, Robert Wood Johnson Medical School, University of Medicine and Dentistry of New Jersey, Piscataway, New Jersey 08854-5635, and Center for Advanced Biotechnology and Medicine and Department of Molecular Biology and Biochemistry, Rutgers University and Robert Wood Johnson Medical School, Piscataway, New Jersey 08854-5638

Received October 11, 2002; Revised Manuscript Received December 10, 2002

ABSTRACT: Coiled coils are well-known as oligomerization domains, but they are also important sites of protein−protein interactions. We determined the NMR solution structure and backbone ^{15}N relaxation rates of a disulfide cross-linked, two-chain, 37-residue polypeptide containing the 34 C-terminal residues of striated muscle α-tropomyosin, $TM9a_{251-284}$. The peptide binds to the N-terminal region of TM and to the tropomyosin-binding domain of the regulatory protein, troponin T. Comparison of the NMR solution structure of $TM9a_{251-284}$ with the X-ray structure of a related peptide [Li, Y., Mui, S., Brown, J. H., Strand, J., Reshetnikova, L., Tobacman, L. S., and Cohen, C. (2002) *Proc. Natl. Acad. Sci. U.S.A. 99*, 7378−7383] reveals significant differences. In solution, residues 253−269 (like most of the tropomyosin molecule) form a canonical coiled coil. Residues 270−279, however, are parallel, linear helices, novel for tropomyosin. The packing between the parallel helices results from unusual interface residues that are atypical for coiled coils. Y267 has poor packing at the coiled-coil interface and a lower R_2 relaxation rate than neighboring residues, suggesting there is conformational flexibility around this residue. The last five residues are nonhelical and flexible. The exposed surface presented by the parallel helices, and the flexibility around Y267 and the ends, may facilitate binding to troponin T and formation of complexes with the N-terminus of tropomyosin and actin. We propose that unusual packing and flexibility are general features of coiled-coil domains in proteins that are involved in intermolecular interactions.

The tropomyosins are two-chain, parallel, α-helical coiled-coil proteins that have long served as paradigms of coiled-coil function and design (*1*, *2*). Here we report the structure of the C-terminal domain of tropomyosin. We propose that its unusual packing and flexibility may be general features of coiled-coil domains in proteins that are involved in intermolecular interactions.

Tropomyosins bind cooperatively to the long pitch grooves of the helical actin filaments in most eukaryotic cells. They are critical for actin filament stabilization and for cooperative regulation of many actin functions (*3*−*5*). Tropomyosin, in association with troponin, cooperatively regulates contraction in response to Ca^{2+} in striated muscle. Mutations in tropomyosin genes encoding sarcomeric tropomyosins cause disease in skeletal and cardiac muscle (*6*, *7*).

In vertebrates, four tropomyosin genes generate more than 20 functionally different isoforms through developmentally regulated and tissue specific exon expression (*4*, *5*). The N- and C-terminal ends of tropomyosin, required for high actin affinity, are encoded by alternatively expressed exons. The ends overlap (*8*) to form continuous cables of tropomyosin along both sides of the actin filament, enabling cooperative interactions.

The C-terminus of tropomyosin in striated muscle (residues 258−284) is encoded by tissue specific expression of exon 9a (*9*). The last 9−11 residues form a complex with the first 9−11 residues of the N-terminus and are needed for cooperative allosteric activation of the actin−tropomyosin filament by myosin (*3*, *10*, *11*). The entire exon 9a-encoded region is required for troponin to promote fully high-affinity actin binding, with the first 18 residues being necessary for the interaction of troponin with tropomyosin in the presence of calcium (*12*). We have proposed that residues 258−276 form a three-chain coiled coil with residues 92−110 of human cardiac troponin T (*13*), a region enriched in mutations that cause hypertrophic cardiomyopathy (*6*).

We report here the three-dimensional NMR solution structure and backbone ^{15}N relaxation rates for a recombinant polypeptide dimer corresponding to the 34 C-terminal amino acids of striated muscle α-tropomyosin obtained at physiological ionic strength. The peptide, $TM9a_{251-284}$,[1] contains the 34 C-terminal residues of α-tropomyosin, with the N279K mutation to increase peptide stability, and the peptide sequence GCG at the N-terminus to allow disulfide cross-

[†] This research was supported by NIH Grant GM-36326 to S.E.H.-D. and N.J.G.

[‡] Coordinates of the structure of $TM9a_{251-284}$ have been deposited with the Protein Data Bank at Rutgers University, New Brunswick, NJ, as entry 1MV4, and the chemical shifts have been deposited with the BMRB at the University of Wisconsin, Madison, WI, under accession number 5610.

* To whom correspondence should be addressed. E-mail: greenfie@umdnj.edu. Telephone: (732) 235-5791. Fax: (732) 235-4029.

[§] University of Medicine and Dentistry of New Jersey.

[||] Rutgers University and Robert Wood Johnson Medical School.

10.1021/bi026989e CCC: $25.00
Published on Web 01/01/2003

linking. The N279K mutation does not change the secondary structure or binding affinity of the peptide for the N-terminus of tropomyosin or troponin T (*13*). In the analysis of the secondary structure, previously reported for this cross-linked polypeptide (*14*), the $^1H^\alpha$ and $^{13}C^\alpha$ chemical shift displacements showed that residues 252−279 are α-helical but residues 280−284 are nonhelical. Significantly, the periodicities of the $^1H^N$ and $^{13}C'$ displacements suggested that residues 257−269 form a coiled coil, but that residues 270−279, while helical, are not in a coiled-coil conformation. The three-dimensional structure reported here is consistent with this secondary structure analysis: residues 253−269 form a canonical coiled coil, but the α-helices formed by residues 270−279 are arranged in an unusual parallel, linear arrangement. In addition, the ^{15}N relaxation rates of the backbone show that the nonhelical C-terminal segment is highly flexible. The flexible C-terminus and the parallel helical regions are interesting because they comprise the binding sites for the N-terminus of tropomyosin and the anchoring region of troponin T, which are both important for the cooperative interactions of tropomyosin. Comparison of the NMR structure of $TM9a_{251-284}$ with the X-ray structure of a related peptide, GCN4-CTm (*15*), reveals significant differences.

MATERIALS AND METHODS

The $TM9a_{251-284}$ peptide was designed, expressed, and purified as previously reported (*14*). The NMR samples were prepared in 100 mM NaCl, 10 mM potassium phosphate, 10% deuterium oxide, and 90% water (pH 6.4). NMR data were collected at 10 °C on a Varian Inova 600 spectrometer (Varian, Inc., Palo Alto, CA). Protein concentrations ranged from 0.5 to 2 mM. The program VNMR (Varian, Inc.) was used for data processing. The program Sparky (T. Goddard and T. Kneller, University of California at San Francisco, San Francisco, CA, unpublished) was used for alignment of the spectra and peak selection.

The assignments of the resonances of the N, H, C^α, C^β, C', and H^α atoms, reported previously (*14*), were determined as described for the N-terminal tropomyosin peptide, GlyTM1bZip (*16*). Distance constraints for the structure analysis of $TM9a_{251-284}$ were obtained by analysis of 3D ^{15}N-edited PFG NOESY-HSQC (*17*, *18*) and ^{13}C-edited PFG NOESY-HSQC (*18*, *19*) experiments, all with mixing times of 100 ms. To distinguish interchain from intrachain distances, a ^{13}C X-filtered experiment was also carried out as described previously (*16*). The NOE cross-peak intensities were then used to estimate an initial set of upper-bound distance constraints as reported previously for GlyTM1bZip (*16*). For the X-filtered spectra, the initial upper limit constraint for each cross-peak was set to 5 Å plus any pseudoatom correction (*20*). The analysis of the constraint data was performed using the programs AutoStructure (*16*, *21*, *22*) and DYANA (*23*) as previously described (*14*). Heteronuclear HNOE spectra and proton-detected ^{15}N longitudinal (R_1) and transverse (R_2) relaxation rates were recorded using pulse sequences and collection parameters similar to those used by Feng et al. (*24*).

Table 1: Summary of Distance Geometry Measurements of $TM9a_{251-284}$

Summary of Experimental Constraints	
no. of NOE-derived upper limit distance constraints per molecule (two chains)	
intrachain total	1414
intraresidue ($i = j$)	650
sequential ($i - j = 1$)	338
medium-range ($1 < i - j \leq 5$)	426
long-range ($i - j > 5$)	0
interchain	234
dihedral angle constraints per molecule[a]	26
hydrogen bond constraints[a]	96

Maximal Constraint Violations in the 10 Best Structures	total	interchain	maximum
upper limit constraint violations (>0.2 Å)	12	0	0.43
van der Waals constraint violations (>0.2 Å)	3	0	0.33
dihedral angle constraint violations	0	0	–

Rmsd Values of Atomic Coordinates of Residues 248−284	
all backbone atoms	1.89 ± 0.46 Å
all heavy atoms	2.02 ± 0.41 Å

Rmsd Values of Atomic Coordinates of α-Helical Residues 254−279	
backbone atoms	0.68 ± 0.29 Å
heavy atoms	1.31 ± 0.26 Å

[a] Dihedral angle constraints ($\theta = -57 \pm 20°$ and $\psi = -47 \pm 20°$) were used for residues where the $^3J(H^N-H^\alpha)$ coupling constants were <6 Hz and the NOE patterns indicated an ideal α-helical conformation. Hydrogen bond constraints were generated on the basis of the NOE constraint patterns using the program AutoStructure (*21*, *22*) as described previously (*16*).

RESULTS

Three-Dimensional Structure of $TM9a_{251-284}$. Analysis of NMR chemical shift data reveals that $TM9a_{251-284}$ is a symmetric dimer (*14*). Further analysis of the ^{13}C- and ^{15}N-edited NOESY spectra and a ^{13}C X-filtered NOESY spectrum using the programs AutoStructure (*16*, *21*, *22*) and DYANA (*25*) gave 1018 assigned nuclear Overhauser effect cross-peaks (NOEs), which were used to derive 1414 intrachain and 234 interchain distance constraints for the two symmetric chains (Table 1), 22.2 distance constraints and 23.9 total constraints per residue. The pattern of the NOEs (*26*) and the chemical shift indices of the H^α, C^α, and C^β chemical shifts (*27*) show that residues 253−279 are α-helical but that the ends are disordered (Figure 1).

[1] Abbreviations: AutoStructure, program for assigning NOESY data and calculating structures from NMR data; 2D, two-dimensional; 3D, three-dimensional; CD, circular dichroism; DYANA, program for computing 3D structures of polypeptides and proteins from NMR data; GCN4, yeast transcriptional activator of amino acid biosynthetic genes; GCN4-CTm, peptide with a N-terminal methionine, followed by residues 255−279 of the GCN4 leucine zipper and then residues 254−284 of rat striated muscle α-tropomyosin; GlyTM1bZip, peptide containing an N-terminal glycine followed by residues 1−19 of tropomyosins with the N-terminus encoded by exon 1b followed residues 264−281 of GCN4; HSQC, heteronuclear single-quantum coherence; NOE, nuclear Overhauser effect; NOESY, NOE spectroscopy; NOE cross-peaks, proton−proton interactions detected in nuclear Overhauser effect spectroscopy; PFG, pulsed-field gradient; rmsd, root-mean-square deviation; $TM9a_{251-284}$, peptide containing a Gly-Cys-Gly sequence followed by residues 251−284 of striated tropomyosin with the C-terminus encoded by exon 9a with the N279K mutation.

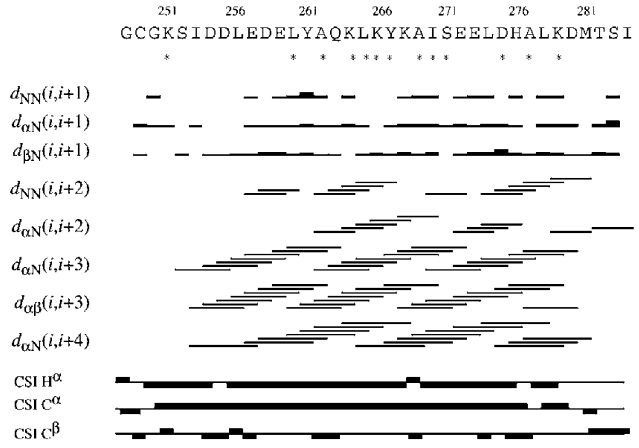

FIGURE 1: Sequential NOEs and chemical shift indices, CSI (*25*), for $TM9a_{251-284}$. The CSI values range from −1 to 1. The starred residues have $^3J(H^N-H^\alpha)$ scalar coupling constants of less than 6 Hz. These data show that residues 252−279 are α-helical but the ends are disordered.

The $TM9a_{251-284}$ peptide is not a typical coiled coil over its entire length (Figure 2). Residues 253−269 of $TM9a_{251-284}$ form a canonical coiled coil with classic knobs-into-holes packing. In contrast, residues 270−279, while showing the NOEs expected for an α-helix, do not form a coiled coil but form unusual *parallel*, *linear* helices. The ribbon depiction of the backbone atoms of $TM9a_{251-284}$ in Figure 2B aligns the two chains to illustrate the parallel region.

The parallel, linear interface of the α-helices of the C-terminus of striated tropomyosin in solution occurs because the sequence of this region is atypical for a coiled coil. In canonical parallel, two-stranded coiled coils, such as that found in the leucine zipper GCN4 (*28*), interface *a* positions in the *abcdefg* heptad repeat typically are *β*-branched hydrophobic amino acids while interface *d* positions are unbranched hydrophobic amino acids (*29*). The C-terminal region of striated tropomyosin, however, has unbranched hydrophobic amino acids in the *a* positions (L260, L288, and M281) as well as a tyrosine (Y267). There are also atypical residues in the *d* positions: Q263, I270, A277, and I284. Gln, Ala, and Tyr residues at the coiled-coil interface reduce stability (*30*). In addition, L278 in an *e* position replaces a usual hydrophilic residue.

The packing of these unusual interface residues has the effect of driving the two helical chains of residues 270−279 to become parallel and linear rather than coiled coil. Most important in this regard are the side chains of L278, in an *e* position, that pack against one another across the helix−helix interface and interact with the side chains of A277 and M281. These atypical interactions are clearly supported by the NMR data. The L278 residues exhibit 13 interchain NOES but the interface *a* and *d* residues in this region of the structure have few interchain NOEs compared to canonical coiled coils. For example, A277 does not pack well with residues from the opposite chain, resulting in only four interchain NOEs compared to 8−15 interchain NOEs for the longer hydrophobic residues at the helix−helix interface. In addition, Y267 and Q263 in the coiled-coil region are poorly packed at the interface with only one and four interchain NOEs, respectively, giving only six and four interchain distances of less than 3.5 Å in the calculated structure. Typically, helix−helix interface residues exhibit 20−40 such interactions. Approximately 30% of the surface area of Y267 is exposed in $TM9a_{251-284}$, reflecting its bulky and polar character (*31*), while the other residues at the helix−helix interface have only 4−10% of their surface area exposed, with the exception of the C-terminal isoleucine.

Backbone Dynamics of $TM9a_{251-284}$. To estimate the relative backbone mobility in the C-terminal region of striated tropomyosin, we obtained the heteronuclear $^1H-^{15}N$ NOEs and R_1 and R_2 ^{15}N relaxation rates for $TM9a_{251-284}$ at 600 MHz and 10 °C. The negative ratios in the HNOE spectra show that the last two residues, S283 and I284, are flexibly disordered (Figure 3A). Residues 280−282 also have lower HNOE ratios than the helical region of the molecule, showing that they are also more mobile, in agreement with the secondary structure predicted by the chemical shift displacements and the relative intensities of the cross-peaks in the HSQC, HNCA, and HNCO spectra (*14*). The relative R_1 and R_2 relaxation rates also indicate that both ends of $TM9a_{251-284}$ are less ordered than the helical domain of the molecule (Figure 3B,C). However, the HNOE spectra and relaxation rates of the amide backbone of the coiled-coil region are similar to those of the parallel helical region of the molecule. The lower R_2 relaxation rates of Y267 and K268 suggest there is conformational exchange broadening in this polypeptide segment, consistent with poor packing of the two Y267 side chains in the coiled coil and consequent local destabilization of the structure. The Q263 side chain amide resonances display conformational heterogeneity in the HSQC (*14*) and NOESY spectra (data not shown), but the backbone shows HNOEs and relaxation rates similar to those of the rest of the helical domain. Similarly, in the Jun homodimer, the Asn side chains at the coiled-coil interface exhibit exchange broadening, but the backbone shows the same dynamic behavior as most of the other coiled-coil residues (*32*).

DISCUSSION

Comparison of the Solution Structure of $TM9a_{251-284}$ with the Crystal Structures of GCN4-CTm and α-Tropomyosin. Comparison of residues 254−284 of the solution structure of $TM9a_{251-284}$ with the crystal structure of a related peptide, GCN4-CTm (*15*) in Figure 2C, shows that the backbones of residues 260−270 of the two structures are in close agreement (rmsd < 1.0 Å). The structures diverge starting at residue 271. In solution, residues 271−279, while not a coiled coil, do form packed parallel helices, whereas those in the crystal structure are splayed apart and interact C-terminus to C-terminus with a second molecule, a nonphysiological association. In solution, there are no NOEs in $TM9a_{251-284}$ consistent with the C-terminal to C-terminal interactions seen in the crystal structure of GCN4-CTm (*15*). Moreover, there is no concentration dependence of either the NMR spectra or circular dichroism of $TM9a_{251-284}$ as a function of temperature, which would be indicative of self-association. The structure of the peptide backbone of $TM9a_{251-284}$ is in closer agreement with that of the low-resolution crystal structure of full-length striated muscle tropomyosin determined at 7 Å (*33*) where the C-termini interact with the N-termini of an adjacent molecule. While not well-resolved in the lower-resolution crystal structure, these residues are not splayed and have the same interchain distances as $TM9a_{251-284}$.

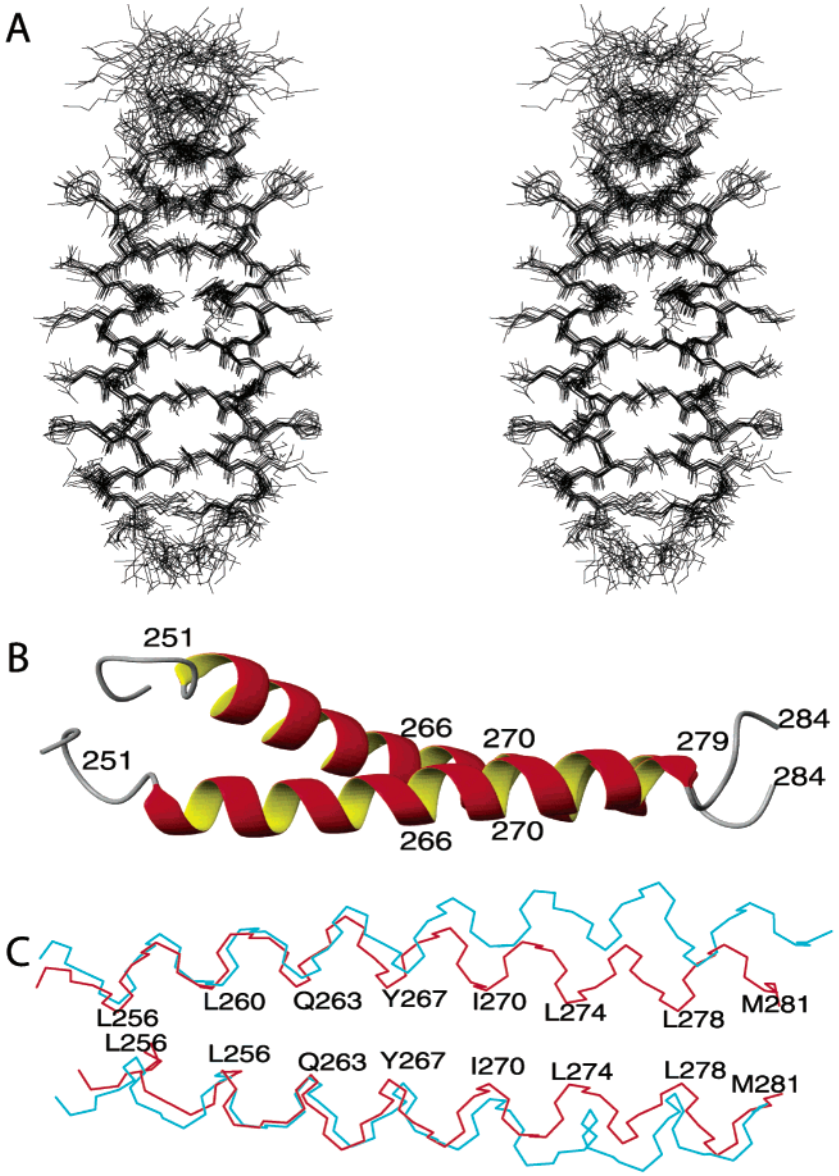

FIGURE 2: (A) Alignment of the heavy atoms of the 10 calculated structures of TM9a$_{251-284}$ giving the lowest upper and van der Waals constraint violations, derived from NOE distance and scalar coupling data using the program AutoStructure. All of the residues are illustrated. The N-terminus is at the top. (B) Ribbon model of all of the residues of TM9a$_{251-284}$ showing that residues 270−279 are in parallel helices. (C) Comparison of the backbone bonds of residues 254−281 from the solution structure of TM9a$_{251-284}$ (red, structure from PDB entry 1MV4) and the crystal structure of GCN4-CTm (blue, PDB entry 1QKL) (*15*). The interface residues are labeled. In each structure, residues 270−279 are helical, but in the crystal structure, the ends are splayed and form a C-terminus−C-terminus complex with another symmetric peptide (not shown). In the solution structure, the residues of the two chains pack against each other to form parallel helices and the peptides do not self-associate.

The splaying of the helices in GCN4-CTm begins at residue Y267, which is poorly packed in the solution structure of TM9a$_{251-284}$. Moreover, in solution the R_2 relaxation rate of the backbone ^{15}N atom of this residue indicates exchange broadening due to conformational flexibility. The crystal structure of the GCN4-CTm dimer illustrates the importance of the flexibility of the C-terminal domain of tropomyosin for its binding interactions. Flexibility would allow the region around Y267 to act as a hinge. In GCN4-CTm, this hinge opens and allows the non-coiled-coil helical region to bind to another molecule, in this case in a tail-to-tail nonphysiological arrangement.

Implications of the Structure of TM9a$_{251-284}$ for Tropomyosin Function. The structure and dynamics of TM9a$_{251-284}$ are different from those of the N-terminal region of tropomyosin, the only other part of tropomyosin known at atomic resolution. Whereas the N-terminal residues in solution form a continuous coiled coil that starts at the first residue when the molecule is N-terminally acetylated (*34*, *35*), the last five residues at the C-terminus are nonhelical and relatively flexible. The parallel helical complex formed by residues 270−279 is novel for tropomyosin. The C-terminal region of tropomyosin is the critical binding site for the N-terminal region of tropomyosin and for troponin T, and the exposed surface presented by the parallel helices may facilitate binding.

The structures of the C-terminus in the overlap complex with the N-terminus and in the ternary complex with the N-terminus and troponin T are unknown. Preliminary circular dichroism data and ^{15}N−^{1}H HSQC (*14*) and ^{15}N-edited NOESY data (N. J. Greenfield, unpublished observations) show that while the chemical shifts of the nitrogen atoms

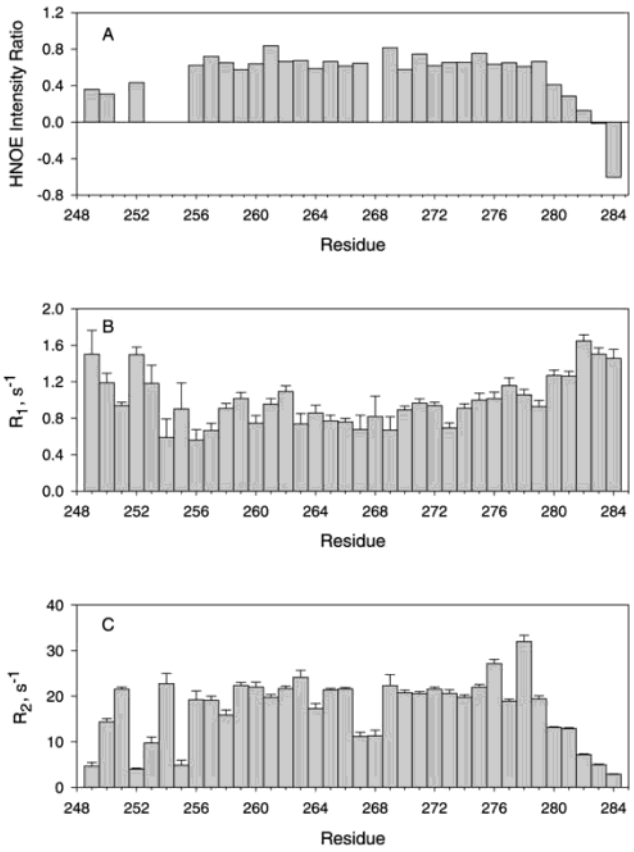

FIGURE 3: Plots of the distribution of (A) $^1H-^{15}N$ heteronuclear NOEs, (B) proton-detected ^{15}N longitudinal relation rates (R_1), and (C) proton-detected ^{15}N transverse relaxation rates (R_2) of $TM9a_{251-284}$ at 600 MHz and 10 °C. The results show that the ends of the molecule are relatively disordered compared to helical residues 256−279, with evidence for conformational exchange broadening around Y267. The missing peaks in panel A were either very broad or overlapped in both of the HNOE spectra collected both with and without broad-band amide proton saturation. Because the $TM9a_{251-284}$ peptide is a rigid rod that tumbles slowly and nonisotropically, and because several of the resonances were broadened, no further attempt was made to fully characterize the internal dynamics.

from the amino acids in the overlap region are displaced upon binding to the N-terminus, there are only minor changes in the H^{α} and H^{N} chemical shifts, suggesting there is little change in secondary structure, although the complexed molecule is more stable. Binding of a troponin T fragment, however, results in large changes in structure. The helical content of the ternary complex increases compared to that of the unmixed components, and the $^{15}N-^{1}H$ HSQC spectrum of the C-terminal region is greatly perturbed.

The solution structure of the C-terminal segment of tropomyosin gives weight to our argument that the flexibility of the coiled-coil region is highly important for function. The side chains of the Q263 residues are mobile, and their conformation changes upon complex formation with the N-terminus and with a troponin T fragment (*14*). Mutations of Q263 that alter the interface packing and stability show the importance of the flexibility of the C-terminus for binding target proteins. A Q263L mutation increases the stability of $TM9a_{251-284}$ but profoundly inhibits its ability to form a ternary complex with the N-terminus of tropomyosin and troponin T, while the Q263A mutation has little effect on stability or binding (*14*). These results suggest that the unusual packing of the Q263 and Y267 side chains, and the conformational exchange of the backbone near Y267, lead to increased flexibility, which is critical for binding to the regulatory protein, troponin T.

A General Hypothesis Regarding Interactions of Coiled-Coil Domains. From our results, and those of others, we present a general hypothesis regarding coiled-coil function. We suggest that flexibility and noncanonical packing may be essential for their binding interactions. A precedent for this idea comes from the crystal structure of an Xrcc4−DNA ligase IV complex, where the exposed surface of the two parallel helices of Xrcc4 binds a single ligase molecule (*36*). A similar structure is found the nucleotide exchange factor GrpE where two long, parallel helices extend away from the globular domain and are postulated to interact with the peptide binding domain of the molecular chaperonin DnaK (*37*). As well as its importance for the interactions of tropomyosin (*14*), the flexibility of coiled-coil regions has been shown to be essential for the interactions and function of other coiled coils such as viral fusion proteins (*38*) and the kinesin family of motor proteins (*39*). Stable, canonical coiled coils may function primarily as oligomerization motifs, whereas less stable or noncanonical coiled coils, such as those seen in an alanine repeat of tropomyosin (*34*), or parallel α-helices as reported here, may serve as binding sites for other molecules.

ACKNOWLEDGMENT

We thank Rajan K. Paranji for his assistance in the interpretation of the molecular relaxation data, Helen Berman for useful discussions, and Barbara Brodsky and Gail Arnold for critically reading the manuscript.

REFERENCES

1. Cohen, C., and Parry, D. A. (1990) *Proteins 7*, 1−15.
2. Hodges, R. S., Saund, A. K., Chong, P. C., St.-Pierre, S. A., and Reid, R. E. (1981) *J. Biol. Chem. 256*, 1214−1224.
3. Gordon, A. M., Homsher, E., and Regnier, M. (2000) *Physiol. Rev. 80*, 853−924.
4. Perry, S. V. (2001) *J. Muscle Res. Cell Motil. 22*, 5−49.
5. Lin, J. J., Warren, K. S., Wamboldt, D. D., Wang, T., and Lin, J. L. (1997) *Int. Rev. Cytol. 170*, 1−38.
6. Bonne, G., Carrier, L., Richard, P., Hainque, B., and Schwartz, K. (1998) *Circ. Res. 83*, 580−593.
7. Laing, N. G. (1999) *Curr. Opin. Neurol. 12*, 513−518.
8. McLachlan, A. D., and Stewart, M. (1975) *J. Mol. Biol. 98*, 293−304.
9. Ruiz-Opazo, N., and Nadal-Ginard, B. (1987) *J. Biol. Chem. 262*, 4755−4765.
10. Lehrer, S. S., and Geeves, M. S. (1998) *J. Mol. Biol. 277*, 1081−1089.
11. Moraczewska, J., and Hitchcock-DeGregori, S. E. (2000) *Biochemistry 39*, 6891−6897.
12. Hammell, R. L., and Hitchcock-DeGregori, S. E. (1996) *J. Biol. Chem. 271*, 4236−4242.
13. Palm, T., Graboski, S., Hitchcock-DeGregori, S. E., and Greenfield, N. J. (2001) *Biophys. J. 81*, 2827−2837.
14. Greenfield, N., Palm, T., and Hitchcock-DeGregori, S. E. (2002) *Biophys. J. 83*, 2754−2766.
15. Li, Y., Mui, S., Brown, J. H., Strand, J., Reshetnikova, L., Tobacman, L. S., and Cohen, C. (2002) *Proc. Natl. Acad. Sci. U.S.A. 99*, 7378−7383.
16. Greenfield, N. J., Huang, J. H., Palm, T., Swapna, G. V. T., Monleon, D., Montelione, G. T., and Hitchcock-DeGregori, S. E. (2001) *J. Mol. Biol. 312*, 833−847.
17. Driscoll, P. C., Clore, G. M., Marion, D., Wingfield, P. T., and Gronenborn, A. M. (1990) *Biochemistry 29*, 3542−3556.

18. Pascal, S. M., Muhandiram, D. R., Yamazaki, T., Forman-Kay, J. D., and Kay, L. E. (1994) *J. Magn. Reson., Ser. B 103*, 197−201.
19. Ikura, M., Kay, L. E., and Bax, A. (1990) *Biochemistry 29*, 4659−4667.
20. Wüthrich, K., Billeter, M., and Braun, W. (1983) *J. Mol. Biol. 169*, 949−961.
21. Montelione, G. T., Zheng, D., Huang, Y. J., Gunsalus, K. C., and Szyperski, T. (2000) *Nat. Struct. Biol.* 7 (Suppl.), 982−985.
22. Huang, Y. J. (2001) Automated determination of protein structures from NMR data by iterative analysis of self-consistent contact patterns, Ph.D. Thesis, Rutgers University, New Brunswick, NJ.
23. Güntert, P., Mumenthaler, C., and Wüthrich, K. (1997) *J. Mol. Biol. 273*, 283−298.
24. Feng, W., Tejero, R., Zimmerman, D. E., Inouye, M., and Montelione, G. T. (1998) *Biochemistry 37*, 10881−10896.
25. Koradi, R., Billeter, M., Engeli, M., Guntert, P., and Wuthrich, K. (1998) *J. Magn. Reson. 135*, 288−297.
26. Wüthrich, K. (1986) *NMR of Proteins and Nucleic Acids*, Wiley, New York.
27. Wishart, D. S., and Sykes, B. D. (1994) *J. Biomol. NMR 4*, 171−180.
28. Landschulz, W. H., Johnson, P. F., and McKnight, S. L. (1988) *Science 240*, 1759−1764.
29. Harbury, P. B., Zhang, T., Kim, P. S., and Alber, T. (1993) *Science 262*, 1401−1407.
30. Wagschal, K., Tripet, B., Lavigne, P., Mant, C., and Hodges, R. S. (1999) *Protein Sci. 8*, 2312−2329.
31. Eisenberg, D., Weiss, R. M., and Terwilliger, T. C. (1982) *Nature 299*, 371−374.
32. MacKay, J. P., Shaw, G. L., and King, G. F. (1996) *Biochemistry 35*, 4867−4877.
33. Whitby, F. G., and Phillips, G. N., Jr. (2000) *Proteins 38*, 49−59.
34. Brown, J. H., Kim, K. H., Jun, G., Greenfield, N. J., Dominguez, R., Volkmann, N., Hitchcock-DeGregori, S. E., and Cohen, C. (2001) *Proc. Natl. Acad. Sci. U.S.A. 98*, 8496−8501.
35. Greenfield, N. J., Montelione, G. T., Farid, R. S., and Hitchcock-DeGregori, S. E. (1998) *Biochemistry 37*, 7834−7843.
36. Sibanda, B. L., Critchlow, S. E., Begun, J., Pei, X. Y., Jackson, S. P., Blundell, T. L., and Pellegrini, L. (2001) *Nat. Struct. Biol. 8*, 1015−1019.
37. Harrison, C. J., Bohm, A. A., and Nelson, H. C. (1994) *Science 263*, 224−227.
38. Carr, C. M., and Kim, P. S. (1993) *Cell 73*, 823−832.
39. Sablin, E. P., Case, R. B., Dai, S. C., Hart, C. L., Ruby, A., Vale, R. D., and Fletterick, R. J. (1998) *Nature 395*, 813−816.

BI026989E